AD-A158 205 PRE-STACK KIRCHHOFF INVERSION OF COMMON OFFSET DATA(U) 1/1
COLORADO SCHOOL OF MINES GOLDEN CENTER FOR WAVE
PHENOMENA M F SULLIVAN ET AL. 04 JUN 85 CWP-027
UNCLASSIFIED N00014-84-K-0049 F/G 9/2 NL

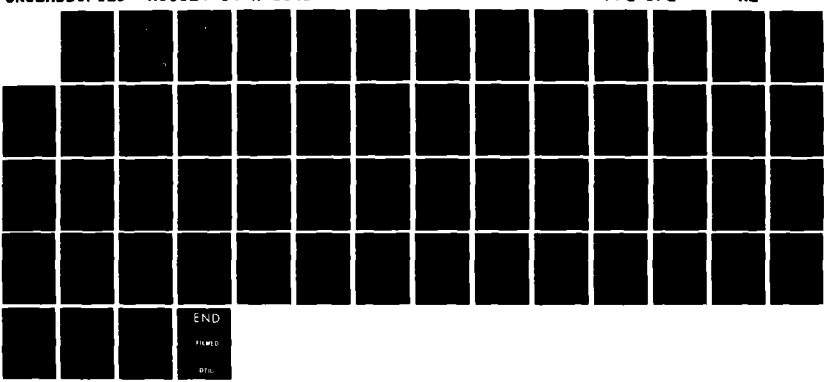

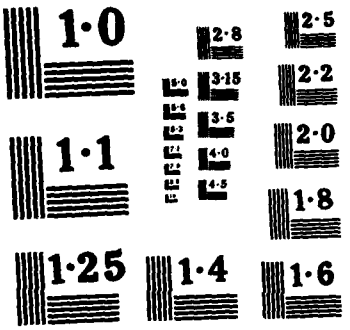

(2)

CSM

PRE-STACK KIRCHHOFF INVERSION OF COMMON OFFSET DATA

by

Michael F. Sullivan and Jack K. Cohen

Partially supported by the Consortium Project of the Center for Wave Phenomena and by the Selected Research Opportunities Program of the Office of Naval Research.

Colorado School of Mines
Golden, Colorado 80401

Center for Wave Phenomena
Department of Mathematics
303/273-3557

CWP-027

PRE-STACK KIRCHHOFF INVERSION OF COMMON OFFSET DATA

by

Michael F. Sullivan and Jack K. Cohen

Partially supported by the Consortium Project of the Center for Wave Phenomena and by the Selected Research Opportunities Program of the Office of Naval Research.

Center for Wave Phenomena
Department of Mathematics
Colorado School of Mines
Golden, Colorado 80401
Phone: (303) 273-3557

TABLE OF CONTENTS

ABSTRACT

A pre-stack inversion algorithm is developed for acoustic Kirchhoff, high-frequency, common offset data. Given the velocity above a reflector, the interface is located and an angularly-dependent reflection coefficient is computed at each reflection point. A quick post-processing step then calculates the velocity of the lower medium. Lateral velocity variations in the second layer are naturally recovered since each reflection point provides an independent measure of the reflection coefficient. The inversion is performed as a mapping where the response to subsurface test points is examined by an integration over the data. If a test point is on the reflector, the reflection coefficient is returned.

Inversion and migration operators both utilize an integral over the data, with each trace in the summation weighted by an amplitude and a phase term. Here, knowledge of an appropriate inversion phase term is gained from a Kirchhoff, high-frequency, forward model. To determine the correct inversion amplitude term, Kirchhoff data for a general surface, in integral form, are entered into the inversion operator. The resulting integral is evaluated via the asymptotic method of 4-dimensional stationary phase. An amplitude term is then chosen so that the inversion operator produces a singular function of support on the reflector, weighted by the reflection coefficient.

The Kirchhoff offset inversion is first formulated for data acquired over a plane, producing a 3-D reflectivity map. Since data are commonly collected along a single line, a 2.5-D specialization is also developed. A method for determining the velocity of the lower medium from an angularly-dependent reflection coefficient is then detailed for the 2.5-D case.

GLOSSARY

A	partial derivative matrix of phase function (22)
$B(\underline{m}, \underline{r}, \underline{r}', c)$	inversion amplitude function (14)
c	compressional velocity (1)
$\underline{d}$	offset variable (B-10)
$g(\omega, \underline{r}, \underline{r}^-)$	free space Green's function (3)
$\underline{h}'(x)$	slope of 2.5-D inversion output interface (58)
$\underline{m}$	source-receiver midpoint location (13)
$\hat{n}$	unit normal vector to reflecting surface (7)
$\underline{r} = (x, y, z)$	cartesians (2)
$\underline{r}' = (x', y', z')$	test point location (14)
$\underline{r}^+$	source location (2)
$\underline{r}^-$	receiver location (3)
R	angularly-dependent reflection coefficient (6)
R^+	source-reflector distance (16)
R^-	reflector-receiver distance (16)
R'^+	source-test point distance (13)
R'^-	test point-receiver distance (13)
$\underline{t}_1$, $\underline{t}_2$	tangent vectors to reflecting surface (18)
$U_k(\omega, \underline{m})$	Kirchhoff observed field , midpoint coodinates (15)
$U_s(\omega, \underline{m})$	observed scattered field , midpoint coordinates(13)
$U_s(\omega, \underline{\xi})$	backscattered field (44)
$U_s(\omega, \underline{r}, \underline{r}^+)$	scattered field due to source at $\underline{r}^+$ (2)
$U_s(\omega, \underline{r}^-, \underline{r}^+)$	observed scattered field (5)
$\underline{\xi} = (\xi, \eta, 0)$	cartesians for backscatter observation point (44)
δ	Dirak delta function (3)

$\varphi(\underline{x})$	phase function (24)
γ^+, γ^-	abbreviation, see (12)
$\underline{\sigma}$	coordinates parameterizing reflecting surface (16)
ω	circular frequency (1)

INTRODUCTION

An inversion method for acoustic pre-stack data provides a means for determining subsurface reflectivity from common shot, common receiver, or common offset time sections. In exploration for hydrocarbons, the areas of greatest interest are those where the geology is the most complicated. As the complexity of the subsurface increases, the validity of the stacked section as an interpretable depth picture decreases. By inverting pre-stack data, a depth reflectivity profile is obtained from each time record.

In all pre-stack methods the reflection coefficient produced is for non-normal incidence. In common shot or common receiver gathers, as the shot-receiver separation increases, so does the angle of the reflected energy. Inversion therefore yields the reflection coefficients as a function of angle, and, with further processing, in a constant density environment, determines velocities below the reflector. Analogously, processing angularly-dependent reflection coefficient data, where velocities are known, recovers densities. Common offset data dictate less angular variation of the reflection coefficient since the separation between source and receiver is fixed at the same constant distance for each experiment.

An important consideration in the selection of an inversion data set is the surface acquisition area. The larger the data collection zone, the greater the delineated portion of the subsurface reflector. In this paper, the development presented is for the inversion of common offset data, for the purpose of recovering sub-reflector velocities. This data set often contains the greatest number of traces, with the largest areal coverage.

Inherent in the definition of any inverse process is an assumption of a specific forward modeling process. Kirchhoff, high-frequency, non-zero

offset modeling for a single arbitrary surface provides the basis of the inversion developed here. Given the compressional wave speed of the first medium, the wave field effects produced by this Kirchhoff data are inverted exactly to yield the interface location and an angularly-dependent reflection coefficient. Each point on the interface has a unique reflection coefficient as a function of angle. Since the offset between the source and receiver is constant for each trace, the incident angle of the energy to each reflection point is determined, and the velocity of the next layer is then computed. With each reflection point independently providing the velocity in the second layer, lateral velocity variations beneath the relector are naturally recovered.

As with migration, inversion is performed by a summation of traces, each weighted by a phase and an amplitude term. The inversion phase term is of opposite sign to the phase used in the Kirchhoff forward model. The amplitude term is an unknown, and is determined by inverting Kirchhoff data, in integral form, from an arbitrary surface. By employing the asymptotic method of 4-dimensional stationary phase, the inversion operator, acting on high-frequency Kirchhoff data, is evaluated. The unknown amplitude function is then selected so that the inversion yields a singular function with support on the reflector, weighted by the reflection coefficient.

The Kirchhoff offset inversion process is intuitively similar to migration, as described by Schneider (1978). The location of a test point is input, and if this test point is on the reflector, the value of the reflection coefficient is returned. For each test point an integral is performed over the common offset traces, with each trace weighted geometrically. The weighted traces add constructively when the position of the test point coincides with the reflecting surface. Since data are not

available at all frequencies, and at all points on the acquisition plane, a band-limited and aperture-limited singular function delineation of the reflector is produced, as demonstrated by Bleistein, Cohen, and Hagin (1985).

The inversion is exact for Kirchhoff, high-frequency data from a single interface. Approximate solutions may be obtained in multi-layer problems by a single pass method or by a layer stripping technique. The accuracy of single pass multi-layer inversion is dependent on the input velocity information, while the error in layer stripping inversion is a function of the ability to downward continue the wave field, preserving amplitudes. Neither method is developed here, however, for completeness, both are described in the context of the derived inversion algorithm.

The inversion algorithm is first formulated for 3-dimensional data sets in which acquisition is over a plane. For this data base, the position of an arbitrary 3-D interface is recovered, along with an angularly-dependent reflection coefficient at each reflection point.

The algorithm is then developed for the 2.5-D case, where data are acquired only along a line. This 2.5-D approximation assumes invariance of geologic structure in the off-line direction, thereby introducing a cylindrical symmetry to the problem. For the 2.5-D specialization, a technique is presented for recovering the velocity of the second layer, given a reflection coefficient from the inversion.

Since the forward model is of such fundamental importance to the inversion development, a complete Kirchhoff, high-frequency modeling derivation preceeds the inversion formulation.

KIRCHHOFF, HIGH-FREQUENCY, NON-ZERO OFFSET MODELING

For the purposes of inversion and simulation of pre-stack data, a forward modeling procedure is required. The Kirchhoff integral method is chosen since it is embedded in wave theory and, as such, produces wave field effects. The development presented here is suited to the modeling of common source, common receiver, or common offset gathers. Of particular interest to the inversion of the next section are data acquired with a constant offset between the source and receiver. The inversion is exact with respect to this Kirchhoff forward model representation.

A high-frequency assumption underlies the forward modeling and inversion theory. The choice of a suitably high frequency is a function of both a distance parameter of the problem, and the velocity of the medium. By assuming that all frequencies of the data are greater than this minimum high frequency, asymptotic evaluations are justified. The distance parameter, r, may be the minimum depth to the reflectors of interest or a "typical" radius of curvature of a reflecting feature. To provide a reasonable approximation, the following relationship must be satisfied:

$$2\omega r/c \gg 1 \quad , \tag{1}$$

where the 2, appearing in equation (1), corresponds to the 2-way travel time of the forward or inverse problem.

For example, if the depth to the reflector is 500 feet in a medium with a compressional wave speed of 10,000 ft/sec, any frequency above 5 Hz is considered suitable since the amplitude error at the low end (5 Hz) of the

frequency spectrum is only a few percent.

The subsequent derivation yields the high-frequency Kirchhoff representation of the wave field reflected from an arbitrary surface. In each experiment the source is offset from the receiver. For modeling purposes, this experiment is repeated along the surface to generate a time section of common offset traces.

The scattered field has its sources on the reflector and is thus governed by the homogeneous wave equation with inhomogeneous boundary conditions:

$$\nabla^2 U_s(\omega, \underline{r}, \underline{r}^+) = 0 \quad . \tag{2}$$

The two spatial variables of the argument of U_s in equation (2) indicate that the recorded value of the scattered field, U_s, at any point $\underline{r}$ is a function of the source position $\underline{r}^+$. Since the scattered field is recorded at only one receiver location, $\underline{r}^-$, per experiment, a sifting operation is performed on the variable $\underline{r}$ of equation (2).

For the purpose of sifting under a volume integral, a second wave equation is introduced:

$$\nabla^2 g(\omega, \underline{r}, \underline{r}^-) + \omega^2/c^2 \; g(\omega, \underline{r}, \underline{r}^-) = - \delta(\underline{r} - \underline{r}^-) \quad . \tag{3}$$

The solution, $g(\omega, \underline{r}, \underline{r}^-)$, is a free space Green's function which describes the propagation of a point source from the location $\underline{r}^-$, toward any point $\underline{r}$. Reciprocity permits $\underline{r}$ and $\underline{r}^-$ to switch places, providing another

representation of equation (3):

$$\nabla^2 g(\omega, \underline{r}^-, \underline{r}) + \omega^2/c^2 \; g(\omega, \underline{r}^-, \underline{r}) = -\delta(\underline{r} - \underline{r}^-) \quad . \tag{4}$$

The physical situation is now that of a wave traveling from any point source location, $\underline{r}$, toward a receiver location, $\underline{r}^-$. In a volume integral context, equation (4) describes a sifting function at the receiver location, and propagates energy from a reflector to the receiver.

The wave field due to a source at $\underline{r}^+$ and a receiver at $\underline{r}^-$, $U_s(\omega, \underline{r}^-, \underline{r}^+)$, is obtained in the following manner: multiply equation (2) by $g(\omega, \underline{r}^-, \underline{r})$ and equation (4) by $U_s(\omega, \underline{r}, \underline{r}^+)$, subtract one result from the other, integrate over a volume of space bounded by the reflector which contains the source and receiver points, and apply Green's second theorem. This yields

$$U_s(\omega, \underline{r}^-, \underline{r}^+) = \iint dS \left[U_s(\omega, \underline{r}, \underline{r}^+) \frac{\partial g(\omega, \underline{r}^-, \underline{r})}{\partial n} - g(\omega, \underline{r}^-, \underline{r}) \frac{\partial U_s(\omega, \underline{r}, \underline{r}^+)}{\partial n} \right] \quad , \tag{5}$$

where the normal vector is pointing inward, and the closed surface is composed of two parts: the reflector truncated at its intersection by a large hemisphere having its base on the reflector.

The scattered field is given exactly by equation (5) as a function of frequency, and source and receiver location. To compute $U_s(\omega, \underline{r}^-, \underline{r}^+)$, the scattered field and its normal derivative on the reflector are needed.

An approximate solution for the scattered field near the reflector, due to an incident point source, has the following form:

$$U_s(\omega, \underline{r}, \underline{r}^+) \sim R \frac{\exp[(i\omega/c)|\underline{r} - \underline{r}^+|]}{4\pi|\underline{r} - \underline{r}^+|} \quad , \tag{6}$$

where R is the geometrical optics, angularly-dependent reflection coefficient. A derivation of this high-frequency reflection coefficient is presented in Appendix A. The derivation follows that of Bleistein (1984) and is included for the reader's convenience.

The high-frequency approximation of the normal derivative of the scattered field is given by

$$\frac{\partial U_s(\omega, \underline{r}, \underline{r}^+)}{\partial n} \sim -(i\omega/c)\,(\nabla|\underline{r} - \underline{r}^+|\cdot\hat{n})\,R\,\frac{\exp[(i\omega/c)|\underline{r} - \underline{r}^+|]}{4\pi|\underline{r} - \underline{r}^+|} \quad . \tag{7}$$

The free space Green's function solution to equation (4) is

$$g(\omega, \underline{r}^-, \underline{r}) = \frac{\exp[(i\omega/c)|\underline{r}^- - \underline{r}|]}{4\pi|\underline{r}^- - \underline{r}|} \quad , \tag{8}$$

and for high frequencies its normal derivative is approximated by

$$\frac{\partial g(\omega, \underline{r}^-, \underline{r})}{\partial n} \sim (i\omega/c)(\nabla|\underline{r}^- - \underline{r}|\cdot\hat{n})\,\frac{\exp[(i\omega/c)|\underline{r}^- - \underline{r}|]}{4\pi|\underline{r}^- - \underline{r}|} \quad . \tag{9}$$

Employing the Sommerfeld radiation condition, the integration over the

hemisphere is neglected. A high frequency approximation for the scattered field is now obtained from equation (5):

$$U_s(\omega, \underline{r}^-, \underline{r}^+) \sim$$

$$\iint dS \left[R \frac{\exp[(i\omega/c)|\underline{r} - \underline{r}^+|]}{4\pi|\underline{r} - \underline{r}^+|} (i\omega/c)(\nabla|\underline{r}^- - \underline{r}|\cdot\hat{\underline{n}}) \frac{\exp[(i\omega/c)|\underline{r}^- - \underline{r}|]}{4\pi|\underline{r}^- - \underline{r}|} \right.$$

$$\left. + R \frac{\exp[(i\omega/c)|\underline{r}^- - \underline{r}|]}{4\pi|\underline{r}^- - \underline{r}|} (i\omega/c)(\nabla|\underline{r} - \underline{r}^+|\cdot\hat{\underline{n}}) \frac{\exp[(i\omega/c)|\underline{r} - \underline{r}^+|]}{4\pi|\underline{r} - \underline{r}^+|} \right] \quad .(10)$$

After evaluating the gradient terms, the scattered field due to an offset source-receiver experiment is written as

$$U_s(\omega, \underline{r}^-, \underline{r}^+) \sim \frac{i\omega}{16\pi^2} \iint dS \; R[\gamma^+ + \gamma^-] \frac{\exp[(i\omega/c)\{\,|\underline{r} - \underline{r}^+| + |\underline{r}^- - \underline{r}|\,\}]}{|\underline{r} - \underline{r}^+||\underline{r}^- - \underline{r}|} \quad ,(11)$$

where

$$\gamma^{\pm} = + \frac{1}{c}(\nabla|\underline{r} - \underline{r}^{\pm}|\cdot\hat{\underline{n}}) = + \frac{(\underline{r} - \underline{r}^{\pm})\cdot\hat{\underline{n}}}{c|\underline{r} - \underline{r}^{\pm}|} \quad . \qquad (12)$$

Equation (11) provides a high-frequency Kirchhoff wave field response for non-zero offset modeling. For each source-receiver geometry, a surface integration produces a single trace. Time sections are then constructed by moving the source and/or receiver in the desired fashion.

3-D INVERSION OPERATOR DEVELOPMENT

An inversion operator is developed for application on pre-stack common offset data, producing a subsurface map of the reflector, along with its reflection coefficients. In general, a reflector is delineated by examining the operator response of many different subsurface test points. For each test point an integral is performed over the data acquisition surface, with each differential contribution of the integral corresponding to a geometrically weighted trace. When a test point is on the reflector, an angularly-dependent reflection coefficient is output. The velocity below each reflection point is then determined by a quick post-inversion processing step. Spatial and temporal sampling combined with finite acquisition area and recording time dictate a band-limited and aperture-limited singular function representation of the interface. The peak amplitude occurs on the reflector and is proportional to the reflection strength.

The inversion operator that is derived has the following form:

$$W[U_s(\omega,\underline{m})] = \iint d\underline{m}^2 A(c,\omega,R'^+,R'^-)\exp[(-i\omega/c)(R'^+ + R'^-)]U_s(\omega,\underline{m}) = \delta(s)\ R \quad .(13)$$

The frequency domain version of the input data is represented by $U_s(\omega,\underline{m})$, with the vector $\underline{m}$ parameterizing the midpoint associated with each experiment. R'^+ is the distance between the source and the test point, and R'^- is the distance from the test point to the receiver. The singular function, $\delta(s)$, acts when the difference between the test point position and

the true reflection position equals zero. Figure 1 illustrates the parameters of the problem, with variable definitions provided in Table 1.

The derivation of the forward modeling equation provides insight as to the form of the inversion operator. In the forward problem, each trace is viewed as a weighted sum of image sources on a reflector. Thus, inversion of forward data to determine the interface location must involve a weighted sum of the recorded surface traces. Also, the idea of propagating back to sources, in migration or inversion, necessitates an inverse phase term. With this in mind, an educated guess of the inversion operator is made:

$$W[U_s(\omega,\underline{m})] = \iint d\underline{m}^2 \int d\omega\ (-i\omega)B(\underline{m},\underline{r},\underline{r}',c)\exp[(-i\omega/c)(R'^{+} + R'^{-})]U_s(\omega,\underline{m}) \quad , (14)$$

where $B(\underline{m},\underline{r},\underline{r}',c)$ is an unknown function containing whatever terms were left out of the guess. This unknown function is determined by substituting in known analytic Kirchhoff data, $U_k(\omega,\underline{m})$, for a single interface in integral form, and then requiring that the following inversion goal be realized asymptotically:

$$W[U_k(\omega,\underline{m})] = \delta(s)\ R \quad . \qquad (15)$$

Upon inserting the Kirchhoff data of equation (11) into the inversion operator defined in equation (14), the following relationship is obtained:

$$W[U_k(\omega, \underline{m})] = \delta(s) \; R =$$

$$\frac{1}{16\pi^2} \iint dm^2 \iint d\sigma^2 \int d\omega \left[\omega^2 \sqrt{g} \; B(\underline{m}, \underline{r}, \underline{r}', c) \; \frac{R[\gamma^+ + \gamma^-]}{R^+ R^-} \right.$$

$$\left. \cdot \quad \exp\left[(i\omega/c)[(R^+ + R^-) - (R'^+ + R'^-)] \right] \right] \quad . \tag{16}$$

Note that the differential surface element of equation (11) is functionally represented as

$$dS = \sqrt{g} \; d\sigma_1 \; d\sigma_2 \quad , \tag{17}$$

where σ_1, σ_2 are the curvilinear coordinates that parameterize the reflecting surface. With $\underline{t}_1$, defined as the tangent vector to curves of constant σ_2, and $\underline{t}_2$ defined as the tangent vector to constant σ_1 curves,

$$\sqrt{g} = |\underline{t}_1 \times \underline{t}_2| \quad . \tag{18}$$

The integral in equation (16) is evaluated via the asymptotic method of stationary phase. Since the forward model is a high-frequency Kirchhoff representation, there is no further assumption necessary at this point. In particular, the integrals over $\underline{\sigma}$ and $\underline{m}$ are performed by 4-dimensional stationary phase, with the integral over ω providing the singular function of arclength along a curve normal to the reflector. The unknown function, $B(\underline{m}, \underline{r}, \underline{r}', c)$ is then chosen such that the relationship in equation (16) is

obtained:

$$W[U_k(\omega, \underline{m})] = \delta(s)\ R \quad . \tag{15}$$

Given an integral of the form

$$I(\alpha) = \int f(\underline{x})\ \exp[i\alpha\phi(\underline{x})]\ d\underline{x} \quad , \ \underline{x} = (x_1, x_2, x_3, \cdots, x_m) \quad , \tag{19}$$

containing a point at which the phase $\phi(\underline{x})$ is stationary, the asymptotic representation for large α is given by:

$$I(\alpha) \sim \left[\frac{2\pi}{\alpha}\right]^{\frac{m}{2}} \quad f(\underline{x}_0)\ \frac{\exp[i\alpha\phi(\underline{x}_0) + i(\text{sgn } A)\pi/4]}{\sqrt{|\det A|}} \quad . \tag{20}$$

The point of stationarity, $\underline{x}_0$, is determined by the condition:

$$\nabla\phi(\underline{x}_0) = 0 \quad . \tag{21}$$

The matrix A, at the stationary point, is defined as

$$A_{jk} = \frac{\partial^2 \phi(\underline{x}_0)}{\partial x_j\ \partial x_k} \qquad j,k = 1,2,3,\cdots,m \tag{22}$$

and

$$\text{sgn } A = 2r - m \quad , \tag{23}$$

where r is the number of positive eigenvalues of A, m is the order of the

matrix, and m-r is the number of negative eigenvalues. The difference in the number of positive and negative eigenvalues is therefore equal to sgn A. It is shown in Appendix C that no eigenvalues are equal to zero on the reflector for the Kirchhoff inversion problem. Since det A equals the product of the eigenvalues, an eigenvalue of zero would nullify the validity of the simple stationary point asymptotic integral representation of equation (20).

For the stationary phase evaluation of equation (16), the phase is taken as

$$\phi(\underline{x}) = \left[\left[R^{+} + R^{-} \right] - \left[R'^{+} + R'^{-} \right] \right] \quad , \tag{24}$$

and the formal large parameter is ω/c. The stationary point of the phase is located where the following four stationary conditions are satisfied:

$$\frac{\partial \phi}{\partial \sigma_i} = 0 \quad , \; i=1,2 \tag{25}$$

and

$$\frac{\partial \phi}{\partial m_i} = 0 \quad , \; i=1,2 \quad . \tag{26}$$

Details concerning the derivation of each partial derivative in the stationary conditions and in the matrix A are provided in Appendix B.

The conditions of stationarity of the phase are as follows:

$$\frac{\partial \phi}{\partial \sigma_i} = 0 \qquad \text{implies} \qquad \hat{R}^+ \cdot \underline{t}_i = \hat{R}^- \cdot \underline{t}_i \quad , \; i=1,2 \quad , \tag{27}$$

$$\frac{\partial \phi}{\partial m_i} = 0 \qquad \text{implies} \qquad \frac{\left[x_i - (m_i - d_i) \right]}{R^+} - \frac{\left[(m_i + d_i) - x_i \right]}{R^-}$$

$$= \frac{\left[x' - (m_i - d_i) \right]}{R'^+} - \frac{\left[(m_i + d_i) - x'_i \right]}{R'^-} \quad . \tag{28}$$

Equation (27) is a form of Snell's law which reaffirms that important contributions from the integral come from specular points.

The matrix A is expressed as

$$A = \begin{bmatrix} \dfrac{\partial^2 \phi}{\partial \sigma_i \, \partial \sigma_j} & \dfrac{\partial^2 \phi}{\partial \sigma_i \, \partial m_j} \\ \dfrac{\partial^2 \phi}{\partial m_i \, \partial \sigma_j} & \dfrac{\partial^2 \phi}{\partial m_i \, \partial m_j} \end{bmatrix} , \tag{29}$$

where each partial derivative is a 2-by-2 matrix.

In the asymptotic evaluation of the integral, the determinant of A must be calculated. As is subsequently demonstrated, the delta function of equation (16) acts as $R'^{\pm}$ approaches $R^{\pm}$, thereby simplifying the calculations. This is analogous to the test point approaching the reflection spot. From Appendix B, it is seen that when $R'^{\pm} = R^{\pm}$,

$$\frac{\partial^2 \phi}{\partial m_i \partial m_j} = 0 \qquad i=1,2,\ j=1,2 \quad . \tag{30}$$

Therefore, in calculating the determinant only those terms which do not vanish are included, yielding

$$\sqrt{|\det A|} = \left| \det \frac{\partial^2 \phi}{\partial \sigma_i \partial m_j} \right| \qquad i=1,2,\ j=1,2 \quad . \tag{31}$$

It can be demonstrated from equation (B-29) that

$$\sqrt{|\det A|} = z \sqrt{g}\ \frac{(R^+ + R^-)(R^{+2} + R^{-2})(1 - \hat{R}^+ \cdot \hat{R}^-)}{(R^+ R^-)^3\ |\hat{R}^+ - \hat{R}^-|} \quad . \tag{32}$$

With sgn A shown to be equal to zero in Appendix C, the asymptotic evaluation of equation (16) is written as

$$W[U_k(\omega, \underline{m})] = \delta(s)\ R =$$

$$\frac{c^2\ B(\underline{m}, \underline{r}, \underline{r}', c)\ R\ [\gamma^+ + \gamma^-]\ (R^+ R^-)^2\ |\hat{R}^+ - \hat{R}^-|}{4\ z\ (R^+ + R^-)\ (R^{+2} + R^{-2})\ (1 - \hat{R}^+ \cdot \hat{R}^-)}$$

$$\cdot \int dw\ \exp[(i\omega/c)[(R^+ + R^-) - (R'^+ + R'^-)]] \quad . \tag{33}$$

A few comments are now required to describe the nature of the function $\delta(s)$. In a 1-dimensional example, $\delta[\phi(t)]$ is given as

$$\delta\left[\phi(t)\right] = \delta\left[at\right] = \frac{1}{\left|\frac{\partial\phi(t)}{\partial t}\right|}\,\delta(t) = \frac{1}{|a|}\,\delta(t) \quad . \tag{34}$$

Equation (34) specifies that as t approaches zero, $\delta[\phi(t)]$ approaches a spike, weighted by $1/|a|$. An unweighted delta function is therefore represented as

$$\left|\frac{\partial\phi(t)}{\partial t}\right|\,\delta\left[\phi(t)\right] = \delta(t) \quad . \tag{35}$$

In the 3-dimensional inversion problem, the unknown function, $B(\underline{m}, \underline{r}, \underline{r}', c)$, is obtained such that the inversion operator produces a singular function scaled only by the reflection coefficient. The weighting due to the argument of

$$\delta(\phi) = \delta\left[(R^{+} + R^{-}) - (R'^{+} + R'^{-})\right] \tag{36}$$

must therefore be accounted for. The singular function of equation (36) acts as the test point approaches the reflector along a curve normal to the reflecting surface. The weighting factor is $\partial\phi/\partial n$, and an unweighted singular function, $\delta(s)$, is thus determined:

$$\delta(\phi) = \frac{\delta(s)\left|\hat{R}^{+} - \hat{R}^{-}\right|}{2\left|1 - \hat{R}^{+} \cdot \hat{S}^{-}\right|} \quad , \tag{37}$$

with the variable s denoting arc length.

It must now be shown that there is only one point at which the delta function acts, where $\underline{R}^{\pm} = \underline{R}'^{\pm}$. The stationary phase conditions from the integration over the data acquisition surface are rewritten as

$$\sin\theta_i^{+} + \sin\theta_i^{-} = \sin\theta_i'^{+} + \sin\theta_i'^{-} \tag{38}$$

and

$$\sin\theta_j^{+} + \sin\theta_j^{-} = \sin\theta_j'^{+} + \sin\theta_j'^{+} \quad , \tag{39}$$

with the equations associated with constant y and constant x planes, respectively. Figure 2 illustrates the constant y case, with the angles measured counterclockwise from the vertical, and the vectors, $\underline{R}^{\pm}_i$ and $\underline{R}'^{\pm}_i$, defined as projections onto the plane. Note that if the test point is to the left of the reflection point, $\sin\theta'^{+}_i < \sin\theta^{+}_i$ and $\sin\theta'^{-}_i < \sin\theta^{-}_i$, thereby violating the stationary condition representation of equation (38). Similarly, the test point cannot be to the right of the reflection point. It must therefore be inside or on the border of the triangle bounded by $\underline{R}^{+}_i$ and $\underline{R}^{-}_i$. An analogous argument in the constant x plane projection indicates that the test point lies inside or on the border of a rectangular cone with an apex at (x,y,z), and vertices of $(m_1-d_1, m_2+d_2, 0)$, $(m_1-d_1, m_2-d_2, 0)$, $(m_1+d_1, m_2-d_2, 0)$, and $(m_1+d_1, m_2+d_2, 0)$. Finally, equality of distances within

the argument of the delta function requires that the test point coincide with the reflection point for the delta function to act.

In order to solve for the unknown function, $B(\underline{m}, \underline{r}, \underline{r}', c)$, the integral over frequency is rewritten in the following form:

$$\int d\omega \exp\left[(i\omega/c)\left[(R^{+} + R^{-}) - (R'^{+} + R'^{-})\right]\right] = 2\pi c\delta\left[(R^{+} + R^{-}) - (R'^{+} + R'^{-})\right]$$

$$= \frac{\pi c\delta(s)\left|\hat{R}^{+} - \hat{R}^{-}\right|}{(1 - \hat{R}^{+} \cdot \hat{R}^{-})} \quad . \tag{40}$$

Noting that

$$[\gamma^{+} + \gamma^{-}] = \frac{2(\hat{R}^{-} \cdot \hat{R}^{+} - 1)}{c\left|\hat{R}^{+} - \hat{R}^{-}\right|} \quad , \tag{41}$$

the value of the unknown function is now obtained as

$$\sigma(\underline{m}, \underline{r}, \underline{r}', c) = -\frac{2z(R^{+} + R^{-})(R^{+2} + R^{-2})(1 - \hat{R}^{+} \cdot \hat{R}^{-})}{\pi c^{2}\,(R^{+} R^{-})^{2}\left|\hat{R}^{+} - \hat{R}^{-}\right|} \quad . \tag{42}$$

Inserting this function into equation (14), the general 3-D Kirchhoff pre-stack inversion formula is produced:

$$W[U_s(\omega,\underline{m})] \sim \delta(s)\, R \sim$$

$$\frac{iz'}{\pi c^2}\iint dm^2 \int d\omega\ \omega\ \frac{(R'^{+}+R'^{-})(R'^{+2}+R'^{-2})\sqrt{2(1-\hat{R}'^{+}\cdot\hat{R}'^{-})}}{(R'^{+}R'^{-})^2}$$

$$\cdot\ \exp[(-i\omega/c)(R'^{+}+R'^{-})]U_s(\omega,\underline{m}) \quad . \tag{43}$$

Since the singular function acts when the test point is on the reflector, $R^{\pm}$ is replaced by $R'^{\pm}$. The angularly-dependent reflection coefficient and the location of the interface are therefore determined by employing equation (43) on common offset data. Within a depth zone of interest, the response of each test point is determined. If the input point is on the interface, the reflection coefficient is returned. Each differential contribution of the surface integral is a geometrically weighted common offset trace in the frequency domain. The spatial range of integration is reduced by estimating the maximum dip of the reflector.

The 3-D backscatter inversion result is obtained as a special case when the offset, $\underline{d}$, equals zero ($R^{\pm} = R'^{\pm}$):

$$W[U_s(\omega,\underline{\xi})] = \frac{8iz'}{\pi c^2}\iint\frac{d\xi^2}{R'^{+}}\int d\omega\ \omega\ \exp(-2i\omega R'^{+}/c)\,{}_sU\ (\omega,\underline{\xi}) = \delta(s)\, R \quad . \tag{44}$$

This checks with the backscatter result of Bleistein, Cohen, and Hagin (1985). In particular, after an integration by parts is performed on equation (42) of Bleistein, et al (1985), equation (44), above, is obtained. The necessary integration by parts is described in Bleistein, et al (1985) in transforming equation (26) to equation (27).

Extensions of the method to the more realistic case of a multi-layered earth are possible. One approach is that of layer stripping in which one "major" reflector is inverted for with each pass through the algorithm. Given the velocity of the uppermost layer, the initial inversion produces the location of the shallowest reflector and the velocity of the next layer. The wave field is then downward continued from the acquisition surface to the initial reflector with a procedure such as that demonstrated by Berryhill (1984). This initial reflector then acts as the acquisition surface and another inversion is completed. Problems still to be addressed in this procedure include that of amplitude preservation during the downward continuation, and the recognition of "suitable" layers. An alternate approach calls for a single pass through the algorithm. For this technique, the velocity employed at each differential integration contribution varies, corresponding to velocities along raypaths connecting each test point to source and receiver positions. A velocity profile is therefore required as input to a single pass multi-layer Kirchhoff inversion.

2.5-D INVERSION OPERATOR SPECIALIZATION

In those cases where data collection is along a single line, a unique solution to the inverse problem is not possible unless off-line reflector information is known. An assumption commonly made is that the direction of data acquisition represents the direction of subsurface geologic variation. This introduces a cylindrical symmetry to the problem, indicating that all parallel data lines would produce an identical time section. Under this 2.5-D assumption, the inversion double integral can be specialized to a single spatial integration along the data collection line. The integral in the off-line, invariant direction is performed by the asymptotic method of 1-dimensional stationary phase.

For the 2.5-D simplification, the data are taken along a line in which the m_1 coordinate varies, and the m_2 coordinate is fixed. The reflector is thus assumed to be a function of x only. Snell's law for this cylindrical surface dictates that the y-value of all specular reflection points is identical. Analogously, in the inversion operator, the important part of the m_2 integration (the stationary point) is the part directly over the specular reflection line.

With data collected along a line of constant m_2, an integral of the following form is considered:

$$I(\alpha) = \int dm_2 \; f(m_2) \; \exp[i\alpha\phi(m_2)] \quad . \tag{45}$$

The asymptotic representation for large α is

$$I(\alpha) \sim f(y') \left[\frac{2\pi}{|\alpha\phi''(y')|}\right]^{1/2} \exp\{i\alpha\phi(y') + i[\operatorname{sgn} \phi''(y')]\ \pi/4\ (\operatorname{sgn} \alpha)\} \quad , (46)$$

where y' is the stationary point.

In the particular case of equation (43), the phase is

$$\phi(m_2) = R'^{+} + R'^{-} \tag{47}$$

and the stationary point satisfies

$$\frac{\partial \phi}{\partial m_2} = (m_2 - y') \left[\frac{1}{R'^{+}} + \frac{1}{R'^{-}} \right] = 0 \quad , \tag{48}$$

ie. $m_2 = y'$. The second derivative of the phase and its sign at the stationary point are also required for the evaluation of the m_2 integral:

$$\phi''|_{y'} = \frac{\partial}{\partial m_2}\left[(m_2 - y')\left[\frac{1}{R'^{+}} + \frac{1}{R'^{-}}\right]\right]_{y'} = \left[\frac{1}{R'^{+}} + \frac{1}{R'^{-}}\right]_{y'} \tag{49}$$

and

$$\operatorname{sgn} \phi''|_{y'} = +1 \quad . \tag{50}$$

With the above information, the 2.5-D Kirchhoff inversion operator is

written as

$$W[U_s(\omega,m_1)] \sim \frac{iz'}{\pi c^2}\int dm_1 \int d\omega\ \omega \frac{(R'^{+} + R'^{-})(R'^{+2} + R'^{-2})}{(R'^{+}R'^{-})^2}\sqrt{2(1-\hat{R}'^{+}\cdot\hat{R}'^{-})}$$

$$\cdot \exp\left[(-i\omega/c)(R'^{+}+R'^{-}) + (i\pi/4)\,\mathrm{sgn}(-\omega/c)\right]\left[\frac{2\pi}{\left|\frac{-\omega}{c}\left[\frac{1}{R'^{+}}+\frac{1}{R'^{-}}\right]\right|}\right]^{1/2} . \quad (51)$$

Since

$$\omega = (\mathrm{sgn}\ \omega)|\omega| = |\omega|\exp[(i\pi/2) - (i\pi/2)(\mathrm{sgn}\ \omega)]$$
$$= i|\omega|\exp[-(i\pi/2)(\mathrm{sgn}\ \omega)] \quad , \quad (52)$$

the 2.5-D Kirchhoff common offset inversion operator is given by

$$W[U_s(\omega,m_1)] \sim$$

$$\frac{-2z'}{\pi^{1/2}c^{3/2}}\int dm_1 \int d\omega\ |\omega|^{1/2}\ \frac{(R'^{+}+R'^{-})^{1/2}(R'^{+2}+R'^{-2})}{(R'^{+}R'^{-})^{3/2}}\sqrt{(1-\hat{R}'^{+}\cdot\hat{R}'^{-})}$$

$$\cdot \exp\left[(-i\omega/c)(R'^{+}+R'^{-}) - (i3\pi/4)(\mathrm{sgn}\ \omega)\right] U_s(\omega,m_1) \quad , \quad (53)$$

where R'^{+} and R'^{-} are evaluated at the stationary point:

$$R'^{+} = \left[[x' - (m_1 - d_1)]^2 + z'^2\right]^{1/2} \quad , \quad (54)$$

$$R'^{-} = \left[[(m_1 + d_1) - x']^2 + z'^2\right]^{1/2} \quad . \quad (55)$$

For each test point, an integration is performed over the data acquisition

line. If the test point is on the reflector, the angularly-dependent reflection coefficient is output.

The inversion produces a reflectivity-depth section, where each x', z' interface coordinate has a unique reflection coefficient associated with its unique incident energy angle. Computation of the lower layer velocity at any reflection point necessitates the measurement of the interface slope, $h'(x)$, from the inversion section.

With the upper layer velocity, c, known, and densities assumed constant, Appendix A provides a relationship for the lower layer velocity, c_1:

$$c_1 = \left[\gamma_t^2 - \gamma_i^2 + c^{-2}\right]^{-1/2}, \tag{56}$$

where

$$\gamma_i = \frac{\hat{n} \cdot \hat{R}^+}{c} \tag{A-26}$$

and

$$\gamma_t = \frac{(1 - R)}{(1 + R)} \gamma_i \quad . \tag{57}$$

The normal, $\hat{n}$, is given by

$$\hat{n} = \frac{h'(x)\hat{i} - \hat{k}}{\left[1 + h'^2(x)\right]^{1/2}} \quad , \tag{58}$$

leading to

$$\gamma_i = \frac{\frac{1}{c}\left[h'(x) \left[x - (m_1 - d_1)\right] - z \right]}{\left[\left[x - (m_1 - d_1)\right]^2 + z^2 \right]^{1/2} \left[1 + h'^2(x)\right]^{1/2}} \quad . \tag{59}$$

The midpoint, m_1, associated with the reflection experiment must be determined. From equation (B-8), the stationary condition is

$$\hat{R}^+ \cdot \hat{n}'(x) = \hat{R}^- \cdot \hat{n}'(x) \quad , \tag{60}$$

providing

$$\frac{\left[x - (m_1 - d_1)\right]\hat{i} + z\hat{k}}{\left[\left[x - (m_1 - d_1)\right]^2 + z^2 \right]^{1/2}} \cdot \frac{\hat{i} + h'(x)\hat{k}}{\left[1 + h'^2(x)\right]^{1/2}} =$$

$$\frac{\left[x - (m_1 + d_1)\right]\hat{i} - z\hat{k}}{\left[\left[x - (m_1 + d_1)\right]^2 + z^2 \right]^{1/2}} \cdot \frac{\hat{i} + h'(x)\hat{k}}{\left[1 + h'^2(x)\right]^{1/2}} \quad . \tag{61}$$

The midpoint coordinate is solved for, yielding:

$$m_1 = x - \frac{z\left[1 - h'^2(x)\right] - \sqrt{z^2\left[1 + h'^2(x)\right]^2 + 4h'^2(x)\, d_1^2}}{2h'(x)} \quad . \tag{62}$$

The velocity is therefore determined in the following manner: select an interface point where the lower layer velocity is to be determined, measure $h'(x)$ from the inversion depth section, calculate m_1 from equation (62), calculate γ_i from equation (59), calculate γ_t from equation (57), and finally, obtain c_1 from equation (56). Lateral velocity variations are

mapped by determining the lower medium velocity from a range of reflection points along the interface.

To determine velocities from a 3-D inversion output, slopes are measured in two orthogonal directions. Two relationships similar to equation (61) are produced, in two unknowns, m_1 and m_2. Once m_1 and m_2 are determined, c_1 is obtained, employing a 3-component normal vector.

CONCLUSIONS

A pre-stack inversion operator has been developed for common offset data. Given the velocity above the reflector, the interface location and its reflection coefficients are determined. A data set acquired over a plane yields a 3-D reflectivity map of the interface. When data are available along a line, it is assumed that the data collection is in the direction of geologic variation. A 2.5-D cylindrically symmetric reflectivity mapping is then obtained. Given reflection coefficients, a quick post-processing step determines sub-reflector velocities after measuring interface slopes off of the inversion output depth sections.

The inversion is exact for Kirchhoff, high frequency, common offset data from experiments *over a single reflector*. If the reflector is 500 feet deep in a medium with a compressional wave speed of 10,000 ft/sec, any frequency information greater than 5 Hz is suitable as input.

There are several extensions to the single interface inversion method that could address the multi-layer problem. The following suggested ideas, however, neglect multiples. One approach is to assume that each layer is independent of all other layers. In this case the inversion errors are sensitive to the choice of a single " above reflector" velocity. Another method is to provide multi-layer velocity information, and then employ Snell's law. Travel times along raypaths

connecting each test point with all source and receiver positions are then computed. This, however, requires knowledge of subsurface velocities. A final idea is that of layer stripping. The initial inversion yields the location of the first reflector. A wave equation downward continuation of the data is then performed to this reflector. The subsequent inversion velocity is determined from the reflection coefficient and an inversion to the next reflector is completed. The layer stripping method, however, assumes that the data are of such quality that layers are discernible across the section. Also, a downward continuation procedure is required for pre-stack data which preserves amplitudes.

ACKNOWLEDGMENT

The authors gratefully acknowledge the support of the Office of Naval Research, Mathematics Division, through its Selected Research Opportunity Program, and the Consortium Project on Seismic Inverse Methods For Complex Structures at the Center for Wave Phenomena, Colorado School of Mines. Consortium members are Amoco Production Company, Conoco, Inc., Digicon Geophysical Corp., Geophysical Exploration Company of Norway A/S, Golden Geophysical Corp., Marathon Oil Company, Mobil Research and Development Corp., Phillips Petroleum Company, Sun Exploration and Research, Texaco USA, Union Oil Company of California, and Western Geophysical.

REFERENCES

Berryhill, J. R., 1984, "Wave-equation datuming before stack": Presented at the 54th Annual International SEG Meeting, Atlanta, Georgia

Bleistein, N., 1984, Mathematical Methods for Wave Phenomena: Academic Press, New York.

Bleistein, N., Cohen, J. K., Hagin, F. G., 1985, "Computational and asymptotic aspects of velocity inversion": Center for Wave Phenomena Research Report, CWP-004, revised: January 31, 1985.

Cohen, J. K., and Bleistein, N., 1983, "The influence of out-of-plane surface properties on unmigrated time sections": Geophysics, v. 48, p. 125-132.

Schneider, W. A., 1978, "Integral formulation for migration in two and three dimensions": Geophysics, v. 43, p. 49-76.

APPENDIX A: ANGULARLY-DEPENDENT REFLECTION COEFFICIENT

The angularly-dependent reflection coefficient, R, is determined under the assumption that the surface appears locally planar to incoming and outgoing energy. This is a high-frequency approximation which permits the calculation of R via plane wave analysis, under the conditions of continuity of the field and its normal derivative across the interface.

The frequency domain representation of the incident, reflected, and transmitted field is given by:

$$U_i \sim A_i \exp(i\omega\tau_i) \quad , \tag{A-1}$$

$$U_r \sim A_r \exp(i\omega\tau_r) \quad , \tag{A-2}$$

$$U_t \sim A_t \exp(i\omega\tau_t) \quad . \tag{A-3}$$

Each amplitude term, A, is a function of space and frequency, and τ is the *eikonal function, equalling travel time along the raypath.*

The total field above the reflector is given as

$$U_a = A_i \exp(i\omega\tau_i) + A_r \exp(i\omega\tau_r) \quad , \tag{A-4}$$

and the total field below as

$$U_b = A_t \exp(i\omega\tau_t) \quad . \tag{A-5}$$

Demanding continuity of the field on the reflecting surface requires that

$$A_i \exp(i\omega\tau_i) + A_r \exp(i\omega\tau_r) = A_t \exp(i\omega\tau_t) \quad , \tag{A-6}$$

which is possible only if the phases match on the surface. Therefore the first continuity condition yields

$$A_i + A_r = A_t \quad . \tag{A-7}$$

Continuity of the normal derivative of the field across the surface states that

$$(\nabla A_i + i\omega A_i \nabla\tau_i)\cdot\hat{n} + (\nabla A_r + i\omega A_r \nabla\tau_r)\cdot\hat{n} = (\nabla A_t + i\omega A_t \nabla\tau_t)\cdot\hat{n} \quad . \tag{A-8}$$

The high frequency assumption coupled with the relatively small variations of amplitude yields:

$$A_i\gamma_i + A_r\gamma_r = A_t\gamma_t \quad , \tag{A-9}$$

where

$$\gamma_i = \nabla\tau_i\cdot\hat{n} \quad , \tag{A-10}$$

$$\gamma_r = \nabla\tau_r\cdot\hat{n} \quad , \tag{A-11}$$

$$\gamma_t = \nabla\tau_t\cdot\hat{n} \quad . \tag{A-12}$$

Employing equations (A-7) and (A-9), A_r and A_t are solved for in terms of A_i and the eikonal gradients:

$$A_r = \frac{\gamma_i - \gamma_t}{-\gamma_r + \gamma_t} A_i \quad , \tag{A-13}$$

$$A_t = \frac{\gamma_i - \gamma_r}{-\gamma_r + \gamma_t} A_i \quad . \tag{A-14}$$

It is now necessary to solve for γ_r and γ_t in terms of γ_i. As stated above, the phases must match on the boundary,

$$\tau_i = \tau_r = \tau_t \quad . \tag{A-15}$$

Taking the tangential derivative of equation (A-15) produces

$$\nabla\tau_i \cdot \hat{t}_j = \nabla\tau_r \cdot \hat{t}_j = \nabla\tau_t \cdot \hat{t}_j \quad , j = 1, 2 \quad , \tag{A-16}$$

where $\hat{t}_1$ and $\hat{t}_2$ represent two unit vectors which parameterize the surface. Since the tangential components of the eikonal function gradients match on the interface, the total gradients on the interface are:

$$\nabla\tau_i = \underline{T} + \gamma_i \hat{n} \quad , \tag{A-17}$$

$$\nabla\tau_r = \underline{T} + \gamma_r \hat{n} \quad , \tag{A-18}$$

$$\nabla\tau_t = \underline{T} + \gamma_t \hat{n} \quad , \tag{A-19}$$

where

$$\underline{T} = \sum_{j=1}^{2} (\nabla\tau_i \cdot \hat{t}_j)\, \hat{t}_j \quad . \tag{A-20}$$

Substituting equation (A-1), (A-2), or (A-3) into the homogeneous wave equation yields the eikonal equation

$$|\nabla\tau| = 1/c \quad . \tag{A-21}$$

Therefore, dotting equations (A-17) and (A-18) with $\nabla\tau_i$ and ∇t_r, respectively, gives

$$|\nabla\tau_i|^2 = |I|^2 + \gamma_i^2 = c^{-2} \qquad \text{(A-22)}$$

$$|\nabla\tau_r|^2 = |I|^2 + \gamma_r^2 = c^{-2} \quad . \qquad \text{(A-23)}$$

Since the incident and reflected energy are of opposite sense with respect to the surface normal direction, the following relationship is obtained:

$$\gamma_i = -\gamma_r \quad . \qquad \text{(A-24)}$$

Analogous operations to equations (A-18) and (A-19) provide

$$\gamma_t = \text{sgn}(\gamma_t)\sqrt{c_1^{-2} - c^{-2} + \gamma_i^2} \quad , \qquad \text{(A-25)}$$

where the velocity in the upper medium is c, and the lower medium velocity is c_1. For the current consideration of a two layer, piecewise constant velocity medium

$$\gamma_i = (\hat{n}\cdot\hat{R}^+)/c \quad , \qquad \text{(A-26)}$$

where $\hat{R}^+$ is the unit vector along the raypath from the source point to the reflector.

A_r and A_t are therefore given as

$$A_r = \frac{\gamma_i - \gamma_t}{\gamma_i + \gamma_t} A_i \quad , \tag{A-27}$$

$$A_t = \frac{2\gamma_i}{\gamma_i + \gamma_t} A_i \quad . \tag{A-28}$$

Taking the ratio of the reflected to the incident amplitudes produces the reflection coefficient:

$$R = \frac{A_r}{A_i} = \frac{\gamma_i - \gamma_t}{\gamma_i + \gamma_t} \quad . \tag{A-29}$$

Similarly, the transmission coefficient is

$$T = \frac{A_t}{A_i} = \frac{2\gamma_i}{\gamma_i + \gamma_t} \quad . \tag{A-30}$$

APPENDIX B: STATIONARY PHASE CALCULATIONS

Computation of $\frac{\partial \phi}{\partial \sigma_i}$

The derivative of the phase function with respect to the parameters defining the reflector is given by

$$\frac{\partial \phi}{\partial \sigma_i} = \frac{\partial}{\partial \sigma_i} \left[\left[R^+ + R^- \right] - \left[R'^+ + R'^- \right] \right] \qquad i=1,2 \quad . \qquad \text{(B-1)}$$

Since R'^+ and R'^+ are functions of an independent test point and therefore unrelated to the true reflector, the partial derivative reduces to

$$\frac{\partial \phi}{\partial \sigma_i} = \frac{\partial}{\partial \sigma_i} \left[R^+ + R^- \right] \qquad i=1,2 \quad . \qquad \text{(B-2)}$$

Expanding the first term results in

$$\frac{\partial R^+}{\partial \sigma_i} = \frac{\partial R^+}{\partial x} \frac{\partial x}{\partial \sigma_i} + \frac{\partial R^+}{\partial y} \frac{\partial y}{\partial \sigma_i} + \frac{\partial R^+}{\partial z} \frac{\partial z}{\partial \sigma_i} \qquad i=1,2 \quad , \qquad \text{(B-3)}$$

which is equivalent to

$$\frac{\partial R^+}{\partial \sigma_i} = \nabla R^+ \cdot \underline{t}_i = \hat{R}^+ \cdot \underline{t}_i \quad , i=1,2 \quad . \qquad \text{(B-4)}$$

Analogously,

$$\frac{\partial R^-}{\partial \sigma_i} = \nabla R^- \cdot \underline{t}_i = -\hat{R} \cdot \underline{t}_i \quad , i=1,2 \quad . \tag{B-5}$$

Therefore, the partial derivative of the phase with respect to the variables which parameterize the reflector is

$$\frac{\partial \phi}{\partial \sigma_i} = \hat{R}^+ \cdot \underline{t}_i - \hat{R}^- \cdot \underline{t}_i \quad , \; i=1,2 \quad . \tag{B-6}$$

The first condition of stationarity of the phase is expressed as

$$\frac{\partial \phi}{\partial \sigma_i} = 0 \quad , \; i=1,2 \quad , \tag{B-7}$$

or

$$\hat{R}^+ \cdot \underline{t}_i = \hat{R}^- \cdot \underline{t}_i \quad , \; i=1,2 \quad . \tag{B-8}$$

This relationship states that when evaluating the integral of equation (17), the important contributions come from the specular points associated with Snell's law.

Computation of $\frac{\partial \phi}{\partial m_i}$

The derivative of the phase function with respect to the midpoint variables of the data acquisition surface is given by

$$\frac{\partial \phi}{\partial m_i} = \frac{\partial}{\partial m_i}\left[\left[R^+ + R^-\right] - \left[R'^+ + R'^-\right]\right] \quad , \; i=1,2 \quad . \tag{B-9}$$

Examination of the first two terms provides insight to the entire derivative:

$$\frac{\partial R^+}{\partial m_1} = -\frac{[x - (m_1 - d_1)]}{R^+} \quad , \quad \frac{\partial R^+}{\partial m_2} = -\frac{[y - (m_2 - d_2)]}{R^+}$$

$$\frac{\partial R^-}{\partial m_1} = \frac{[(m_1 + d_1) - x]}{R^-} \quad , \quad \frac{\partial R^-}{\partial m_2} = \frac{[(m_2 + d_2) - y]}{R^-} \quad . \tag{B-10}$$

In a succint notation, the entire partial derivative is written as

$$\frac{\partial \phi}{\partial m_i} = -\frac{[x_i - (m_i - d_i)]}{R^+} + \frac{[(m_i + d_i) - x_i]}{R^-}$$

$$+ \frac{[x_i' - (m_i - d_i)]}{R'^+} - \frac{[(m_i + d_i) - x_i']}{R'^-} \quad , \; i=1,2 \quad . \tag{B-11}$$

where $x_1 = x$, and $x_2 = y$. The second condition of stationarity of the phase is

$$\frac{\partial \phi}{\partial m_i} = 0 \quad , \; i=1,2 \quad , \tag{B-12}$$

or

$$\hat{R}^+ \cdot \hat{i} - \hat{R}^- \cdot \hat{i} = \hat{R}'^+ \cdot \hat{i} - \hat{R}'^- \cdot \hat{i} \quad , \tag{B-13}$$

$$\hat{R}^+ \cdot \hat{j} - \hat{R}^- \cdot \hat{j} = \hat{R}'^+ \cdot \hat{j} - \hat{R}'^- \cdot \hat{j} \quad . \tag{B-14}$$

Computation of $\frac{\partial \phi^2}{\partial \sigma_i \partial \sigma_j}$

The second partial derivative of the phase with respect to reflector parameters is

$$\frac{\partial^2 \phi}{\partial \sigma_i \, \partial \sigma_j} = \frac{\partial}{\partial \sigma_j} \left[(\hat{R}^+ - \hat{R}^-) \cdot \underline{t}_i \right] \quad , \; i=1,2 \; , \; j=1,2 \quad . \tag{B-15}$$

Since $\underline{t}_i$ varies as a function of σ_i

$$\frac{\partial \underline{t}_i}{\partial \sigma_j} = \frac{\partial \underline{t}_i}{\partial \sigma_j} \delta_{ij} \quad , \tag{B-16}$$

where

$$\delta_{ij} = \begin{matrix} 1 & i=j \\ 0 & i \neq j \end{matrix} \quad . \tag{B-17}$$

Therefore,

$$\frac{\partial^2 \phi}{\partial \sigma_i \partial \sigma_j} = \left[\frac{\partial}{\partial \sigma_j}(\hat{R}^+ - \hat{R}^-)\right] \cdot \underline{t}_i + (\hat{R}^+ - \hat{R}^-) \cdot \frac{\partial \underline{t}_i}{\partial \sigma_j} \delta_{ij} \quad . \tag{B-18}$$

Separating the remaining derivatives into two terms yields

$$\frac{\partial \hat{R}^+}{\partial \sigma_j} \cdot \underline{t}_i = \frac{\partial \left[\frac{\underline{R}^+}{R^+}\right]}{\partial \sigma_j} \cdot \underline{t}_i = \frac{1}{R^+}(\underline{t}_j \cdot \underline{t}_i) - \frac{1}{R^+}(\hat{R}^+ \cdot \underline{t}_j)(\hat{R}^+ \cdot \underline{t}_i) \tag{B-19}$$

and

$$\frac{\partial \hat{R}^-}{\partial \sigma_j} \cdot \underline{t}_i = \frac{\partial \left[\frac{\underline{R}^-}{R^-}\right]}{\partial \sigma_j} \cdot \underline{t}_i = -\frac{1}{R^-}(\underline{t}_j \cdot \underline{t}_i) + \frac{1}{R^-}(\hat{R}^- \cdot \underline{t}_j)(\hat{R}^- \cdot \underline{t}_i) \quad . \tag{B-20}$$

Combining all terms, the second partial derivative is obtained:

$$\begin{aligned} \frac{\partial^2 \phi}{\partial \sigma_i \partial \sigma_j} &= \frac{1}{R^+}\left[(\underline{t}_j \cdot \underline{t}_i) - (\hat{R}^+ \cdot \underline{t}_j)(\hat{R}^+ \cdot \underline{t}_i)\right] \\ &+ \frac{1}{R^-}\left[(\underline{t}_j \cdot \underline{t}_i) - (\hat{R}^- \cdot \underline{t}_j)(\hat{R}^- \cdot \underline{t}_i)\right] \\ &+ (\hat{R}^+ - \hat{R}^-) \cdot \frac{\partial \underline{t}_i}{\partial \sigma_j} \delta_{ij} \quad . \end{aligned} \tag{B-21}$$

Computation of $\frac{\partial \phi^2}{\partial \sigma_i \partial m_j}$

The next second partial derivative is taken with respect to both the acquisition surface midpoint variables, and the reflector parameters,

$$\frac{\partial^2 \phi}{\partial \rho_i \, \partial m_j} = \frac{\partial}{\partial m_j} \left[(\hat{R}^+ - \hat{R}^-) \cdot \underline{t}_i \right] \qquad i=1,2 \;, \quad j=1,2 \quad . \tag{B-22}$$

Since the two surfaces are independent of one another the partial derivative is reduced to

$$\frac{\partial^2 \phi}{\partial \sigma_i \, \partial m_j} = \left[\frac{\partial}{\partial m_j} (\hat{R}^+ - \hat{R}^-) \right] \cdot \underline{t}_i \qquad i=1,2 \;, \quad j=1,2 \quad . \tag{B-23}$$

This first term is evaluated as follows:

$$\frac{\partial \hat{R}^+}{\partial m_j} \cdot \underline{t}_i = \left[\frac{1}{R^+} \frac{\partial \underline{R}^+}{\partial m_j} - \frac{1}{R^+} \frac{\partial R^+}{\partial m_j} \hat{R}^+ \right] \cdot \underline{t}_i \qquad j=1,2 \tag{B-24}$$

$$= \frac{1}{R^+} \left[-\hat{j} + \frac{[x_j - (m_j - d_j)]}{R^+} \hat{R}^+ \right] \cdot \underline{t}_i \qquad j=1,2 \quad , \tag{B-25}$$

where $\hat{1}$ is the unit vector in the x-direction and $\hat{2}$ is the unit vector in the y-direction. The second term of the partial derivative is similarly obtained:

$$\frac{\partial \hat{R}^-}{\partial m_j} = \frac{1}{R^-} \left[\hat{j} - \frac{[(m_j + d_j) - x_j]}{R^-} \hat{R}^- \right] \cdot \underline{t}_i \qquad j=1,2 \quad . \tag{B-26}$$

Combining these two terms and noting that

$$\frac{[x_j - (m_j - d_j)]}{R^+} = \hat{R}^+ \cdot \hat{y} \qquad \text{(B-27)}$$

and

$$\frac{[(m_j + d_j) - x_j]}{R^-} = \hat{R}^- \cdot \hat{y} \quad , \qquad \text{(B-28)}$$

the final form of the second partial derivative is

$$\frac{\partial^2 \phi}{\partial \sigma_i \, \partial m_j} =$$

$$\left[\left[\frac{1}{R^+} + \frac{1}{R^-} \right](-\hat{y}) + \frac{1}{R^+}(\hat{R}^+ \cdot \hat{y})\hat{R}^+ + \frac{1}{R^-}(\hat{R}^- \cdot \hat{y})\hat{R}^- \right] \cdot \underline{t}_i \quad i=1,2, \; j=1,2 \; . \qquad \text{(B-29)}$$

Computation of $\frac{\partial \phi^2}{\partial m_i \, \partial m_j}$

The final second partial derivative is

$$\frac{\partial^2 \phi}{\partial m_i \, \partial m_j} = \frac{\partial}{m_j} \left[- \frac{[x_i - (m_i - d_i)]}{R^+} + \frac{[(m_i + d_i) - x_i]}{R^-} \right.$$

$$\left. + \frac{[x_i' - (m_i - d_i)]}{R'^+} - \frac{[(m_i + d_i) - x_i']}{R'^-} \right] \quad i=1,2, \; j=1,2. \qquad \text{(B-30)}$$

Each term is obtained in the same manner, the first is illustrated:

$$\frac{\partial}{\partial m_j}\left[-\frac{[x_i-(m_i-d_i)]}{R^+}\right] =$$

$$\left[-\frac{\partial}{\partial m_j}[x_i-(m_i-d_i)]\right]\frac{1}{R^+} - [x_i-(m_i-d_i)]\frac{\partial\left[\frac{1}{R^+}\right]}{\partial m_j} =$$

$$\frac{\delta_{ij}}{R^+} - \frac{[x_j-(m_j-d_j)][x_i-(m_i-d_i)]}{R^{+3}} \quad . \qquad \text{(B-31)}$$

Upon combining all terms, the second partial derivative is given as :

$$\frac{\partial^2\phi}{\partial m_i\,\partial m_j} = \delta_{ij}\left[\frac{R^+ + R^-}{R^+R^-} - \frac{R'^+ + R'^-}{R'^+R'^-}\right]$$

$$- \frac{[x_j-(m_j-d_j)][x_i-(m_i-d_i)]}{R^{+3}} + \frac{[x'_j-(m_j-d_j)][x'_i-(m_i-d_i)]}{R'^{+3}}$$

$$- \frac{[(m_j+d_j)-x_j][(m_i+d_i)-x_i]}{R^{-3}} + \frac{[(m_j+d_j)-x'_j][(m_i+d_i)-x'_i]}{R'^{-3}}$$

$$i=1,2,\ j=1,2 \quad . \qquad \text{(B-32)}$$

APPENDIX C: SGN A CALCULATION

The value of det A and sgn A are required at the point of action of the singular function. At this point it is seen , from equations (29) and (30), that det A is non-negative, regardless of the shape of the reflector. Furthermore, since $\hat{R}^+$ and $\hat{R}^-$ are of opposite sense, as depicted in Figure 1, equation (32) states that det A is never equal to zero on the reflector. Since det A equals the product of the eigenvalues, this product, $\lambda_1\lambda_2\lambda_3\lambda_4$, is always positive on the reflector. The sign of the eigenvalue product remains unchanged if the sign of any two, or of all four, eigenvalues changes. However, to change sign, an eigenvalue must pass through zero, at which point det A equals zero. Therefore, since det A, on the reflector, is never equal to zero, the sign of each eigenvalue is constant on the reflector, and is not a function of its shape. With the shape of the reflector not influencing the eigenvalue signs, the simplest interface, a flat plane, is employed in calculating sgn A.

For a flat plane, let $\underline{t}_1 = \hat{i}$, $\underline{t}_2 = \hat{j}$, $\sigma_1 = x$, and $\sigma_2 = y$. Without loss of generality, data acquisition is in the x-direction, with $d_2 = 0$ and $d_1 = d$. The stationary conditions specify $m_1 = x$ and $m_2 = y$, yielding

$$R^+ = R^- = R_p = \left[d^2 + z^2\right]^{1/2}, \tag{C-1}$$

$$\hat{R}^+ = \frac{d\hat{i} + z\hat{k}}{R_p}, \tag{C-2}$$

$$\hat{R}^- = \frac{d\hat{i} - z\hat{k}}{R_p}. \tag{C-3}$$

The matrix A is now written as

$$A = \begin{bmatrix} \frac{2}{R_p}\left[1 - \frac{d}{R_p}\right]^2 & 0 & -\frac{2}{R_p}\left[1 - \frac{d^2}{R_p^2}\right] & 0 \\ 0 & \frac{2}{R_p} & 0 & \frac{-2}{R_p} \\ \frac{-2}{R_p}\left[1 - \frac{d^2}{R_p^2}\right] & 0 & 0 & 0 \\ 0 & \frac{-2}{R_p} & 0 & 0 \end{bmatrix} \quad . \qquad \text{(C-4)}$$

To simplify the algebra involved in solving the characteristic equation of matrix A, let the following definitions apply:

$$a = \frac{2}{R_p}\left[1 - \frac{d}{R_p}\right]^2 \quad , \qquad \text{(C-5)}$$

$$b = \frac{2}{R_p}\left[1 - \frac{d^2}{R_p^2}\right] \quad , \qquad \text{(C-6)}$$

$$c = \frac{2}{R_p} \quad . \qquad \text{(C-7)}$$

The eigenvalues are obtained by solving the algebraic equation of degree 4,

$$\det (A - \lambda I) = 0 \quad , \qquad \text{(C-8)}$$

or when expanded:

$$\lambda^4 - (a + c)\lambda^3 + (ac - c^2 - b^2)\lambda^2 + (ac^2 + cb^2)\lambda + (cb)^2 = 0 \quad . \qquad \text{(C-9)}$$

Sgn A is determined from equation (C-9) without explicitly finding the eigenvalues. The product of the eigenvalues is $(cb)^2$. Since this product

is always positive, no eigenvalues are equal to zero. Furthermore, this restricts the signs of the eigenvalues to three cases: all are positive, or all are negative, or there are two of each sign. The sum of the eigenvalues is (a+c), which is also positive. Therefore, not all of the eigenvalues are negative. Finally,

$$-(ac^2 + cb^2) = \sum_{i=1}^{4} \sum_{j=i+1}^{4} \sum_{k=j+1}^{4} \lambda_i \lambda_j \lambda_k \quad , \qquad (C\text{-}10)$$

with $(ac^2 + cb^2)$ always positive, indicates that some of the eigenvalues are negative. Thus, two are positive, two are negative, and sgn A equals zero.

It is possible for sgn A to be nonzero far from the reflector. In the 2-dimensional stationary phase calculations performed in Kirchhoff forward modeling, Cohen and Bleistein (1984) demonstrate that passing through buried foci changes sgn A. The resulting distributions have support on the reflector, with negligible amplitudes far from the reflector. Analogously, foci associated with the 2 surfaces of the inversion problem may produce a nonzero sgn A. However, the large parameter of the asymptotic analysis requires large radii of curvature, placing foci far from the reflector. Therefore contributions of these nonzero sgn A distributions are negligible.

TABLE 1

Integration Parameter Definitions

source location : $\underline{r}^+ = (\underline{\xi}^+, 0) = (\xi^+, \eta^+, 0) = \xi^+\hat{\mathbf{i}} + \eta^+\hat{\mathbf{j}}$

receiver location: $\underline{r}^- = (\underline{\xi}^-, 0) = (\xi^-, \eta^-, 0) = \xi^-\hat{\mathbf{i}} + \eta^-\hat{\mathbf{j}}$

source-receiver midpoint: $\underline{m} = (m_1, m_2, 0)$

offset variable: $\underline{d} = (d_1, d_2, 0)$

source location in midpoint variables: $\underline{r}^+ = (m_1-d_1, m_2-d_2, 0)$

receiver location in midpoint variables: $\underline{r}^- = (m_1+d_1, m_2+d_2, 0)$

reflection point location: $\underline{r} = (x, y, z)$

source-reflector vector: $\underline{R}^+ = \underline{r} - \underline{r}^+ = (x-\xi^+, y-n^+, z)$

reflector-receiver vector: $\underline{R}^- = \underline{r}^- - \underline{r} = (\xi^--x, n^--y, -z)$

test point: $\underline{r}' = (x', y', z')$

source-test point vector: $\underline{R}'^+ = \underline{r}' - \underline{r}^+ = (x'-\xi^+, y'-\eta^+, z')$

test point-receiver vector: $\underline{R}'^- = \underline{r}^- - \underline{r}' = (\xi^- - x', n^--y', -z')$

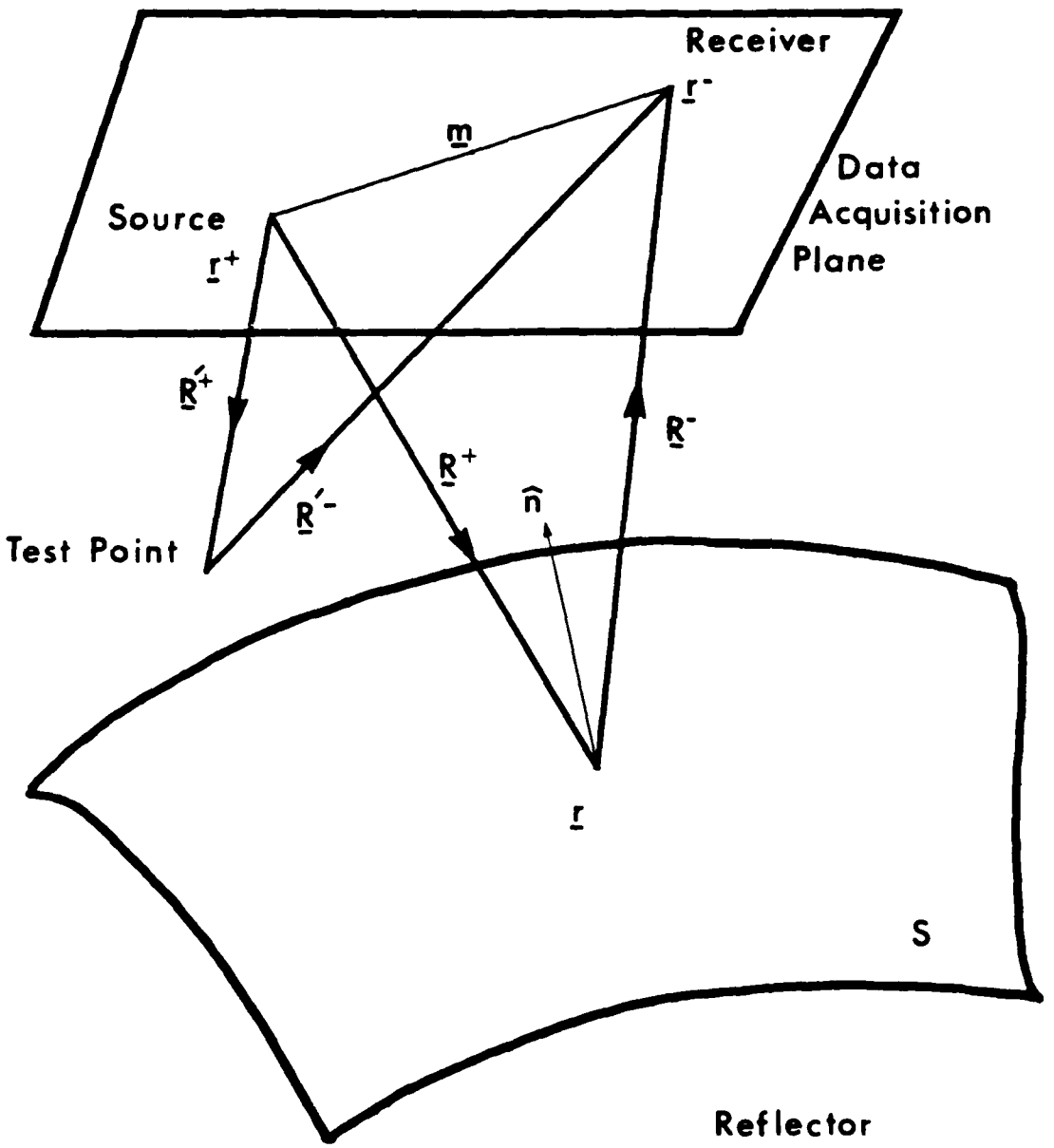
Receiver
$\underline{r}^-$
$\underline{m}$
Data
Acquisition
Plane
Source
$\underline{r}^+$
$\underline{R}'^+$
$\underline{R}^-$
$\underline{R}^+$
$\underline{R}'^-$
$\hat{n}$
Test Point
$\underline{r}$
S
Reflector

Figure 1

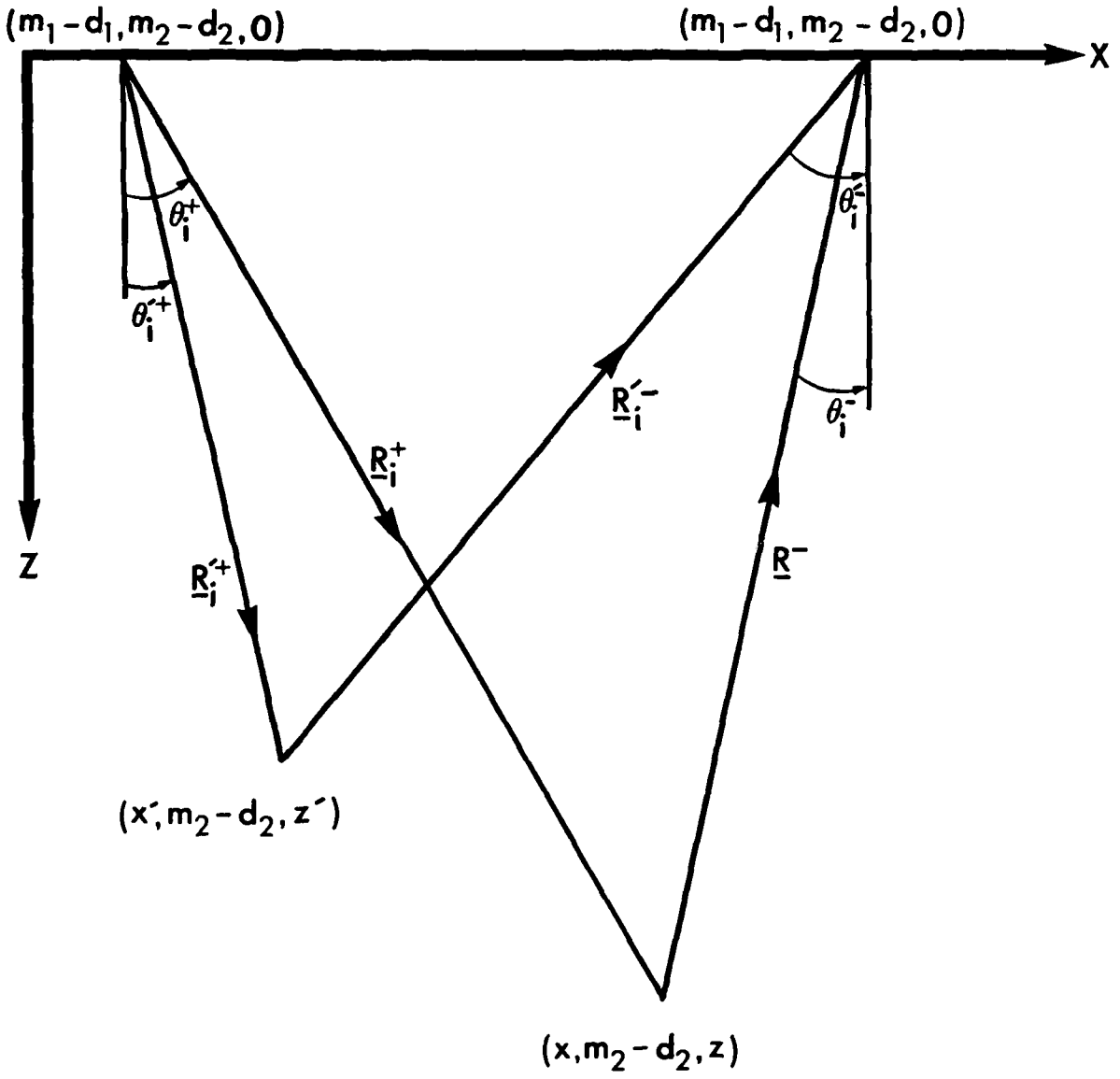
$(m_1 - d_1, m_2 - d_2, 0)$
$(m_1 - d_1, m_2 - d_2, 0)$
X
Z
θ_i^+
$\theta_i'^+$
$\theta_i'^-$
θ_i^-
$\underline{R}_i^+$
$\underline{R}_i'^-$
$\underline{R}_i'^+$
$\underline{R}^-$
$(x', m_2 - d_2, z')$
$(x, m_2 - d_2, z)$

Figure 2

UNCLASSIFIED

SECURITY CLASSIFICATION OF THIS PAGE (When Data Entered)

REPORT DOCUMENTATION PAGE		READ INSTRUCTIONS BEFORE COMPLETING FORM
1. REPORT NUMBER CWP-027	2. GOVT ACCESSION NO. A158 203	3. RECIPIENT'S CATALOG NUMBER
4. TITLE (and Subtitle) Pre-Stack Kirchhoff Inversion of Common Offset Data		5. TYPE OF REPORT & PERIOD COVERED Technical 6. PERFORMING ORG. REPORT NUMBER
7. AUTHOR(s) Michael F. Sullivan Jack K. Cohen		8. CONTRACT OR GRANT NUMBER(s) N00014-84-K-0049
9. PERFORMING ORGANIZATION NAME AND ADDRESS Center for Wave Phenomena Department of Mathematics Colorado School of Mines, Golden, CO 80401		10. PROGRAM ELEMENT, PROJECT, TASK AREA & WORK UNIT NUMBERS NRSRO-159/84APR20(411)
11. CONTROLLING OFFICE NAME AND ADDRESS Office of Naval Research Arlington, VA 22217		12. REPORT DATE 6/4/85 13. NUMBER OF PAGES 55
14. MONITORING AGENCY NAME & ADDRESS(if different from Controlling Office)		15. SECURITY CLASS. (of this report) 15a. DECLASSIFICATION/DOWNGRADING SCHEDULE

16. DISTRIBUTION STATEMENT (of this Report)

This document has been approved for public release and sale; its distribution is unlimited.

17. DISTRIBUTION STATEMENT (of the abstract entered in Block 20, if different from Report)

18. SUPPLEMENTARY NOTES

19. KEY WORDS (Continue on reverse side if necessary and identify by block number)

Pre-Stack Inversion, Kirchhoff Inversion, Common Offset Inversion.

20. ABSTRACT (Continue on reverse side if necessary and identify by block number)

(See reverse side)

DD FORM 1 JAN 73 1473 EDITION OF 1 NOV 65 IS OBSOLETE
S/N 0102-014-6601

SECURITY CLASSIFICATION OF THIS PAGE (When Data Entered)

ABSTRACT

A pre-stack inversion algorithm is developed for acoustic Kirchhoff, high-frequency, common offset data. Given the velocity above a reflector, the interface is located and an angularly-dependent reflection coefficient is computed at each reflection point. A quick post-processing step then calculates the velocity of the lower medium. Lateral velocity variations in the second layer are naturally recovered since each reflection point provides an independent measure of the reflection coefficient. The inversion is performed as a mapping where the response to subsurface test points is examined by an integration over the data. If a test point is on the reflector, the reflection coefficient is returned.

Inversion and migration operators both utilize an integral over the data, with each trace in the summation weighted by an amplitude and a phase term. Here, knowledge of an appropriate inversion phase term is gained from a Kirchhoff, high-frequency, forward model. To determine the correct inversion amplitude term, Kirchhoff data for a general surface, in integral form, are entered into the inversion operator. The resulting integral is evaluated via the asymptotic method of 4-dimensional stationary phase. An amplitude term is then chosen so that the inversion operator produces a singular function of support on the reflector, weighted by the reflection coefficient.

The Kirchhoff offset inversion is first formulated for data acquired over a plane, producing a 3-D reflectivity map. Since data are commonly collected along a single line, a 2.5-D specialization is also developed. A method for determining the velocity of the lower medium from an angularly-dependent reflection coefficient is then detailed for the 2.5-D case.

END

FILMED

10-85

DTIC